Photometric Redshifts and High Redshift Galaxies
ASP Conference Series, Vol. 191, 1999
R.J. Weymann, L.J. Storrie-Lombardi, M. Sawicki, and R.J. Brunner, eds.

Photometric Redshifts Applied to WFPC2 and NICMOS HDF Data

Rodger I. Thompson

Steward Observatory, University of Arizona, Tucson, AZ 85721

Ray J. Weymann and Lisa J. Storrie-Lombardi

Carnegie Observatories, 813 Santa Barbara Street, Pasadena, CA 91101-1292

Abstract. A photometric redshift analysis of optical and infrared images of the Northern Hubble Deep Field indicate a constant star formation rate for redshifts between 1 and 6. The small size of the field and small number of high redshift objects limits this finding to just the area of the NICMOS image. The photometric redshift technique is a modified version of chi square fits to observed and calculated galaxy spectral energy distribution templates.

1. Introduction

The combination of WFPC2 optical and NICMOS infrared observations in the northern Hubble Deep Field (HDF) provides an unsurpassed opportunity to study the history of star formation back to epochs when the universe was on the order of 5% of its present age. The faintness of the sources, however, puts most of them out of the reach of spectroscopic analysis making photometric redshift analysis the only way to determine the redshifts for the majority of sources.

Previous work on the galaxies in the HDF (Madau et al. 1996, Madau 1999) suggested that star formation peaked at a redshift between 1 and 2, then fell off with increasing redshift. Since those studies used the ultraviolet flux at 1500$\AA$ as the measure of the star formation rate, the accuracy of the measurement depends on good knowledge of the extinction in the measured galaxy. Images of the HDF at far infrared wavelengths (Hughes et al. 1998) indicates that a substantial fraction of the emitted ultra violet radiation has been converted by dust absorption to far infrared flux. The true rate of star formation, therefore, may have been seriously underestimated.

Since our observations extend over a factor of 5 in wavelength we have the opportunity to not only measure the photometric redshift but also the photometric extinction. We then use the photometric extinction to correct the ultra violet flux levels in each galaxy and determine an extinction corrected star formation rate. Although this method is an improvement over studies that make no correction for extinction it is still a first step in improving the analysis. Individual galaxies have a very large range of internal extinction and the locations of intense star formation probably have higher extinction values than the average.

2. Observations

Our data comes from observations of the HDF with WFPC2 and NICMOS. The original observations (Williams et al. 1996) provided images at four optical wavelengths of 3000, 4500, 6060, and 8140Å. The deep NICMOS observation of the HDF (Thompson et al. 1999) provided images at 1.1 and 1.6 microns. The NICMOS images, however, only cover a 50 by 50 arc second region in one part of the optical HDF. Our results will pertain only to the region of overlap between the optical and infrared results.

The data reduction for each set of NICMOS observations follows the techniques described in Thompson et al. 1999. However, the photometric values used in the redshift and extinction analyses are 0.6 arc second diameter aperture magnitudes determined by the photometric reduction package SExtractor (Bertin and Arnouts 1996). The object positions determined by the F160W NICMOS image were used as the centers for the flux calculations in all of the other wavelength bands. Objects not detected in the F160W image, therfore, do not appear in this analysis. The SExtractor isophotal and total flux determinations are also recorded. The total flux is utilized in the measurement of the total ultraviolet flux.

3. Photometric Redshift Technique

We utilize a photometric redshift technique that minimizes a modified chi square fit between the observed galaxy and a set of spectral energy distribution (SED) templates which include both observed nearby standard galaxies and calculated templates based on the work of Bruzual and Charlot 1996 and Leitherer et al. 1999. We chose this method over a polynomial fitting technique (Wang, Bahcall, and Turner 1998, Wang, Bahcall, and Turner 1999) since we expect that many of the galaxies will be at high redshifts where adequate training sets of observations do not exist for the polynomial determination.

The basic technique minimizes the chi square residuals between the observed fluxes and those predicted by the various template SEDs which are numerically adjusted for a grid of redshifts and extinctions measured by E(B-V). Our technique differs from that of Fernandez-Soto, Lanzetta and Yahil 1999 and Lanzetta et al. 1996 eg by altering the error to include the flux level as well as the formal error derived from the read noise and dark current. Our chi square residual is given by

$$\chi(z,E)^2 = \sum_{i=1}^{6} \frac{(f_i - A \cdot fmod(z,E)_i)^2}{\sqrt{\sigma_i^2 + f_i^2}} \tag{24}$$

In equation 24 the index i refers to the six fluxes used in this work, f_i is the measured flux and $fmod(z,E)$ is the flux predicted by a template at a redshift of z and with an extinction measured by an E(B-V) value of E. The normalization constant A, is chosen to minimize the value of $\chi(z,E)^2$ and is given by

$$A = \sum_{i=1}^{6} \frac{f_i \cdot fmod(z,E)_i}{\sigma_i^2 + f_i^2} \Big/ \sum_{i=1}^{6} \frac{(fmod(z,E)_i)^2}{\sigma_i^2 + f_i^2} \tag{25}$$

The values of σ_i are calculated from the noise values in the images. The NICMOS values of σ_i are functions of position in the image as discussed in Thompson et al. 1999. At high flux levels the flux error between the observed and model flux divided by the total flux dominates the chi square calculation. At low fluxes it is the flux error divided by the formal sigma that dominates. This formulation acknowledges that the most probable error at high flux levels is a percentage of the flux rather than the formal error determined from low signal level sources or the photon counting statistics.

3.1. Templates

We draw our templates from several sources. The first source is the four observed SEDs of Coleman, Wu, and Weedman 1980 utilized by several authors. The composite SED of Calzetti 1994 and Calzetti 1999 provides an additional observed template of a late type galaxy. The remainder of the templates come from calculations. We use two templates of very young, low metalicity galaxies obtained from the data base of Leitherer et al. 1999. The templates represent 200 million year old galaxies with a metalicity of z = 0.004. One template has instantaneous star formation and the other continuous star formation for 200 million years. The final nonevolving template is a 50 million year old continuous star formation SED calculated from Bruzual and Charlot 1996 models with a Salpeter IMF and solar metalicity. Templates containing equal parts of the Coleman, Wu, and Weedman 1980 early type galaxy and one of the three later types produce 3 composite age SEDs.

We also have 3 evolving templates calculated from the evolutionary models of Bruzual and Charlot 1996. These models have a Salpeter IMF and solar metalicity. All 3 initiate star formation at a redshift of 8 and have instantaneous, continuous, and exponential star formation rates. The decay time for the exponential rate is 1 Gyr. We start star formation at a redshift of 8 because for redshifts greater than 8 all of the flux falls in the F160W band. It is not possible to accurately determine redshifts for objects that have flux only in one band.

3.2. Extinction

For each of the templates we apply a range of extinctions characterized by values of E(B-V) of 0 to 1. The range between 0 and 0.1 is taken in steps of 0.02 and the range between 0.1 and 0.9 in steps of 0.1. We use the work of Calzetti 1994 to determine the extinction as a function of wavelength and the relationship between the value of E(B-V) and the extinction. The final result is 195 different templates in a 13 by 15 grid of intrinsic galaxy SED and extinction.

3.3. Redshift

The chi square value of the fit between an observed galaxy and a template is calculated for 100 different redshifts in a range between 0 and 8 in 0.08 steps for z. The work of Madau 1995 quantifies the obscuration from the Lyman continuum and Lyman lines as a function of redshift. After all of the templates are matched at each redshift, the case with minimum value of chi square is taken as the appropriate redshift, extinction, and intrinsic galaxy SED.

3.4. Star Formation Rate

This work utilizes the relationship between the star formation rate and the ultraviolet flux at 1500$\mathring{A}$ given by Madau, Pozzetti and Dickinson 1998.

$$SFR = 1.25 \times 10^{-28} \cdot UV_{1500} M_{\odot}/yr \tag{26}$$

The units of uv flux in equation 26 are ergs per second per angstrom. This relationship is dependent on the initial mass function (IMF) and therefore may be different at earlier times.

Although the redshifts and extinctions are determined from the 0.6 arc second diameter aperture fluxes, the total ultraviolet flux is determined from the total flux measurement. The total ultraviolet is measured from the ultraviolet flux at 1500$\mathring{A}$ of the selected template both with and without the determined extinction value. The template flux is used because for low redshift values the true 1500$\mathring{A}$ flux is not observed and for higher redshift values the flux is measured through a very wide bandwidth which makes the true 1500$\mathring{A}$ flux difficult to determine. The extincted value is a measure of the observed star formation rate while the unextincted flux measures the star formation rate corrected for extinction. Both values are shown in Figure 1.

4. Results

The results of the analysis are shown in Figure 1. The latest results from Madau 1999 are also shown on the plot as X values without error bars. The error bars on the NICMOS observations indicate the errors expected from photometric errors and in the case of the extinction corrected values both the photometric and extinction errors. Since this is a measure of the star formation rate in the NICMOS portion of the HDF the error bars do not represent counting statistic errors from the often rather small number of galaxies in the bin. These would be relevant only if we were to attempt a determination of the universal star formation rate. The error bars in the redshift are taken to be the width of the bins.

A flat, $H_0 = 50$ cosmology is used to facilitate the comparison with the early work by Madau and others. This is most likely not the correct cosmology but the differences between cosmologies are probably less than the inherent errors in the measurements. The figure has been edited in one manner. The extinction values of galaxies have been limited to an E(B-V) value of 0.2. In some cases a single galaxy with a very high formally determined extinction totally dominated the corrected star formation rate. Before these values are considered real a careful comparison must be made with the far infrared observations. This will be done in later work, however, the observations of Hughes et al. 1998 found no individual far IR sources in the NICMOS field of view.

The net conclusion is that the rate of star formation is roughly constant for redshifts out to 6 and beyond. The rapidly dwindling number of sources beyond 6 make any conclusions in this region very shakey. The results are roughly consistent with the previous work if only the results to a redshift of 4 are considered. The main difference is the maintenance of the star formation rate for redshifts greater than 4. The very small size of the field means that

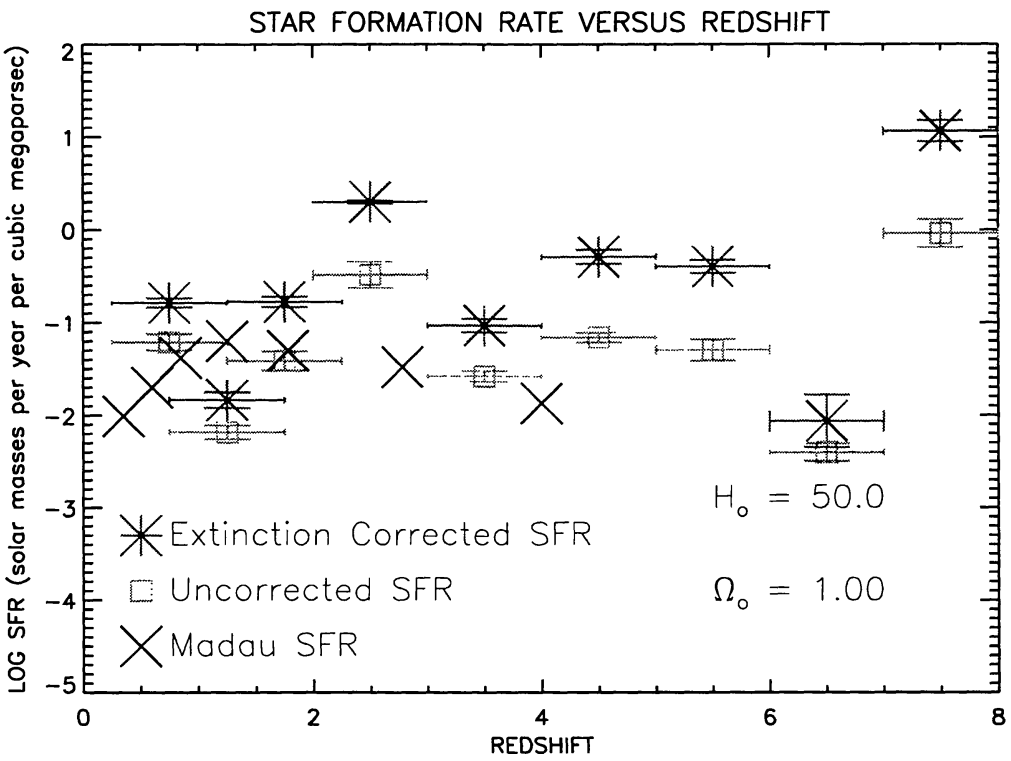

Figure 1. Star Formation as a function of redshift

small scale structure strongly affects the redshift distribution of this particular sample.

Acknowledgments. This work is supported in part by NASA grant NAG 5-3042. This work utilized observations with the NASA/ESA Hubble Space Telescope, obtained at the Space Telescope Science Institute, which is operated by the Association of Universities for Research in Astronomy under NASA contract NAS5-26555.

References

Bertin, E. and Arnouts, S. 1996, A&A, 117, 393

Bruzual, G. and Charlot S., GISSEL96

Calzetti, D. 1999 Private communication of digital data.

Calzetti, D., Kinney, A. L., and Storchi-Bergmann, T. 1994, ApJ, 429, 582.

Coleman, G.D., Wu, C-C, and Weedman, D.W., 1980 ApJS, 43, 393.

Fernandez-Soto, A., Lanzetta, K., and Yahil, A. 1999, ApJ, 513, 34.

Hughes, D., Sergeant, S., Dunlop, J., Rowan-Robinson, M., Blain, A., Mann, R.G., Ivison, R., Peacock, J., Efstathiou, A., Gear, W., Oliver, S.,

Lawrence, A., Longair, M., Goldschmidt, P., and Jenness, T. 1998, Nature, 394, 241.

Lanzetta, K., Yahil, A., and Fernandez-Soto 1996, Nature, 381, 759

Leitherer, C., Schaerer, D., Goldader, J.D., Delgado, R.M.G., Carmelle, R., Kune, D.F., Mello, D.F., Devost, D., and Heckman, T.M. 1999, ApJS, submitted.

Madau, P. 1995, ApJ, 441, 18.

Madau, P. 1999, preprint, astro-ph/9901237.

Madau, P., Ferguson, H.C., Dickinson, M.E., Giavalisco, M., Steidel, C.C., and Fruchter, A. 1996, MNRAS, 283, 1388

Madau, P., Pozzetti, L. and Dickinson, M. 1998,ApJ, 498, 106

Thompson, Rodger I., Storrie-Lombardi, Lisa, J., Weymann, Ray J., Rieke, Marcia, J., Schneider, Glenn, Stobie, Elizabeth, and Lytle, Dyer 1999, AJ, 117, 17.

Wang, Y., Bahcall, N., and Turner, E.L. 1998, AJ, 116, 2081

Wang, Y., Bahcall, N., and Turner, E.L. 1999, this volume

Williams, R.E., Blacker, B. Dickinson, M., Dixon, W.V.D, Ferguson, H.C., Fruchter, A.S., Giavalisco, M., Gilliland, R.L., Heyer, I. Katsanis, R., Levay, Z. Lucas, R.A., McElroy, D.B., Petro, L., Postman, M. Adorf, H-M., and Hook, R.N. 1996, AJ, 112, 1335